# LETTERS

How kinesin waits between steps

Teppei Mori[1], Ronald D. Vale[2] & Michio Tomishige[1,2]

Kinesin-1 (conventional kinesin) is a dimeric motor protein that carries cellular cargoes along microtubules[1,2] by hydrolysing ATP[3] and moving processively in 8-nm steps[4]. The mechanism of processive motility involves the hand-over-hand motion of the two motor domains ('heads')[5–7], a process driven by a conformational change in the neck-linker domain of kinesin[8–12]. However, the 'waiting conformation' of kinesin between steps remains controversial[13–16]—some models propose that kinesin adopts a one-head-bound intermediate[17–21], whereas others suggest that both the kinesin heads are bound to adjacent tubulin subunits[7,22,23]. Addressing this question has proved challenging, in part because of a lack of tools to measure structural states of the kinesin dimer as it moves along a microtubule. Here we develop two different single-molecule fluorescence resonance energy transfer (smFRET) sensors to detect whether kinesin is bound to its microtubule track by one or two heads. Our FRET results indicate that, while moving in the presence of saturating ATP, kinesin spends most of its time bound to the microtubule with both heads. However, when nucleotide binding becomes rate-limiting at low ATP concentrations, kinesin waits for ATP in a one-head-bound state and makes brief transitions to a two-head-bound intermediate as it walks along the microtubule. On the basis of these results, we suggest a model for how transitions in the ATPase cycle position the two kinesin heads and drive their hand-over-hand motion.

The first FRET sensor for distinguishing one-head-bound from two-head-bound states is a kinesin heterodimer in which one polypeptide chain contains a single cysteine residue in the plus-end-oriented tip of the catalytic core (residue 215), and the other chain contains a single cysteine residue in the minus-end-oriented base of the core (residue 43) (sensor termed 215–43; Fig. 1a). The second sensor is a kinesin homodimer in which a cysteine residue was introduced in both chains at the beginning of the neck linker (residue 324) (sensor termed 324–324).

To test our FRET sensors, we first examined the FRET efficiency in a kinesin dimer bound statically to a microtubule with the non-hydrolysable nucleotide analogue AMP-PNP, a nucleotide state in which both kinesin heads are bound to the microtubule[10,17,21,22]. Maleimide-modified Cy3 (donor dye) and Cy5 (acceptor dye) were reacted with the two cysteine residues in these FRET constructs, and single kinesin molecules that contained both Cy3 and Cy5 were selected for smFRET observations with total-internal-reflection fluorescence microscopy[12]. SmFRET efficiencies for the 215–43 sensor from individual microtubule-bound heterodimers showed a bimodal distribution of low (about 10%) and high (about 90%) FRET efficiencies (Fig. 1b), as expected if the two kinesin heads are bound to adjacent tubulin subunits 8 nm apart along a microtubule protofilament (Fig. 1a and Supplementary Figs 1 and 2). Our previous FRET measurements with the 215–43 sensor (Fig. 2e in ref. 12) indicated that the high-FRET peak (about 90%) corresponds to the 43 dye on the leading head and the 215 dye on the trailing head and the low-FRET peak (about 10%) corresponds to the opposite dye
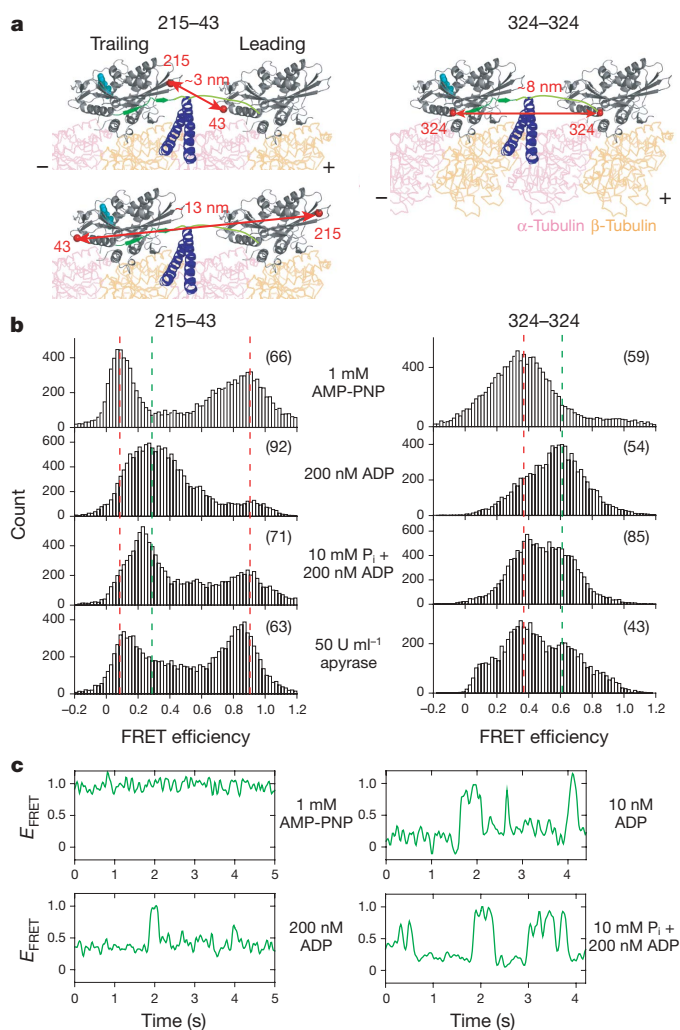
Figure 1 | SmFRET observations of head–head configuration of kinesin under various nucleotide conditions. a, Diagrams of the two-head-bound intermediate state of the kinesin dimer on the microtubule. Positions of cysteine residues for dye labelling are shown in red. The neck linker, neck coiled-coil and bound nucleotide are shown in green, blue and cyan respectively. **b**, Histograms of FRET efficiencies (from each frame of images) of dye-labelled kinesin bound to the axonemes with 1 mM AMP-PNP (ATP-like state), 200 nM ADP, 200 nM ADP/10 mM P_i or 50 U ml^{-1} apyrase (nucleotide-free state). The numbers of molecules analysed are shown in parentheses. Dotted lines illustrate peaks characteristic of putative two-head-bound (red) and one-head-bound (green) states. The correlation of FRET efficiencies with distance measurements is discussed in Supplementary Fig. 1. **c**, Examples of a FRET efficiency (E_{FRET}) trace of individual axoneme-bound 215–43 heterodimer kinesin. ADP and ADP/P_i traces occasionally showed abrupt and large FRET changes (see Supplementary Fig. 4 for additional traces).

[1]Department of Applied Physics, The University of Tokyo, Tokyo 113-8656, Japan. [2]Howard Hughes Medical Institute and Department of Cellular and Molecular Pharmacology, University of California, San Francisco, California 94158, USA.

positioning. The unimodal smFRET distribution centred at about 35% for the 324–324 sensor (Fig. 1b) also is consistent with a two-head-bound state. Binding of the two kinesin heads along a single protofilament (as opposed to sideways across protofilaments) is supported by additional FRET experiments with a 149–324 sensor (Supplementary Fig. 2).

We next examined smFRET under different nucleotide conditions. With ADP occupying the active site, kinesin is in a weak microtubule-binding state[3,18,21]; however, at low ADP concentrations (200 nM) single kinesin dimers remained bound to microtubules for more than 10 s. The FRET histograms at 200 nM ADP clearly differed from those described above for AMP-PNP (Fig. 1b), becoming unimodal and centred at about 30% for the 215–43 sensor and shifting from 35% (AMP-PNP) to 60% for the 324–324 sensor. The result from the 324–324 sensor suggests that the two kinesin heads come closer together. As verified in the experiments described below, these FRET distributions with ADP reflect a one-head-bound state. We next added excess inorganic phosphate (10 mM P_i) to 200 nM ADP, which probably results in partial occupancy of an ADP·P_i state in the tethered head[23]. Under this condition, FRET peaks characteristic of a two-head-bound state appeared (Fig. 1b). Similar results were obtained after the addition of 1 mM AlF_4^- to 1 mM ADP (Supplementary Fig. 3). These results suggest that the addition of P_i or AlF_4^- to ADP-kinesin shifts the equilibrium from a one-head-bound state to a two-head-bound state, as described previously[23]. When both kinesin heads are nucleotide-free (50 U ml^{-1} apyrase; see Methods), the FRET distributions for the 215–43 and 324–324 sensors were generally similar to that observed with AMP-PNP, but with broader distributions (Fig. 1b), suggesting that nucleotide-free kinesin primarily adopts a two-head-bound state (see also ref. 22) with partial occupancy of a one-head-bound state.

Interestingly, whereas the FRET signal of the 215–43 sensor in the presence of 1 mM AMP-PNP was fairly constant, a subset of molecules (about 25%) with ADP or ADP/P_i (Fig. 1c and Supplementary Fig. 4), or under nucleotide-free conditions (not shown) underwent abrupt FRET transitions (from about 30% to either 90% or 10% FRET), which most probably represent unbinding and rebinding events of one of the kinesin heads with the microtubule.

The results from our ADP FRET experiments suggest that kinesin can adopt a one-head-bound state on the microtubule. To obtain additional evidence for this hypothesis, we engineered a kinesin heterodimer in which only one head could bind to microtubules under all nucleotide conditions (mutation Y274A/R278A/K281A in loop 12, termed 'L12-triple')[24,25]. We made two different versions of this heterodimer. SmFRET measurements with a heterodimer containing a 215-labelled dye in the wild-type (WT) polypeptide and a 43-labelled dye in the L12-triple polypeptide, namely 215(WT)–43(L12), produced a unimodal distribution centred at about 30% FRET efficiency with 200 nM ADP (Fig. 2a). Another heterodimer in which the dye positions were reversed in the wild-type and L12-triple chains, namely 215(L12)–43(WT), also showed similar FRET efficiency, indicating that the distances between 43-labelled and 215-labelled dyes are similar in these two configurations. A similar result was obtained in the nucleotide-free state (Fig. 2a), in contrast with the bimodal FRET distribution in wild-type kinesin dimer after nucleotide depletion (Fig. 1b). These results further support the interpretation that a 30% FRET signal of the 215–43 sensor in the presence of ADP is diagnostic of a one-head-bound state.

The FRET histogram for the WT/L12-triple heterodimer changed markedly after the addition of AMP-PNP. For the 215(WT)–43(L12) heterodimer, the histogram became bimodal with the primary peak now emerging at 80% FRET efficiency; for the 215(L12)–43(WT)
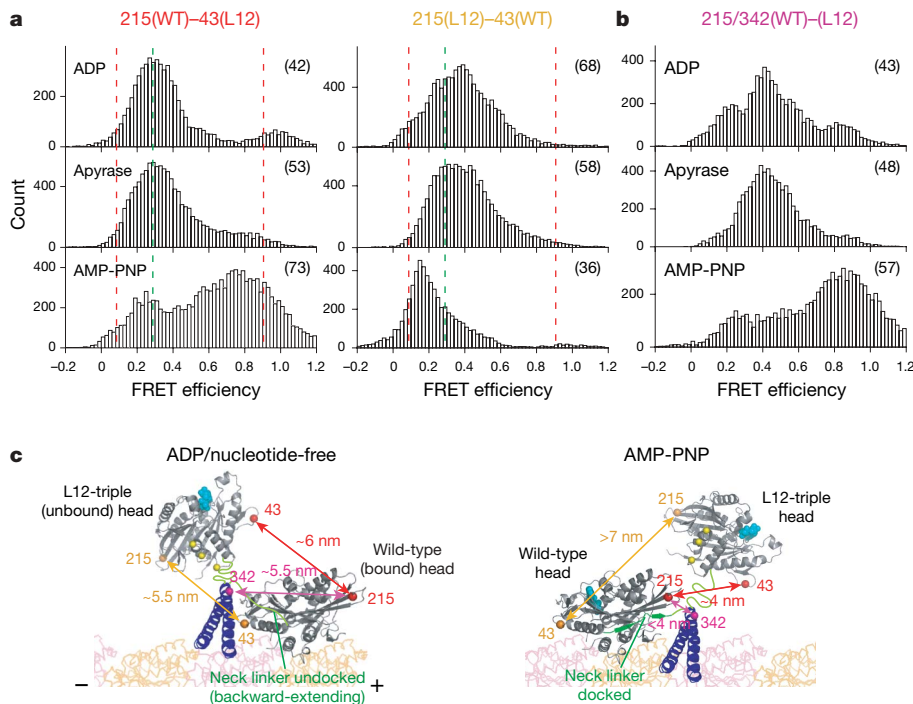
Figure 2 | SmFRET observations of mutant heterodimeric kinesin that persistently takes one-head-bound state. a, Histograms of FRET efficiencies of axoneme-bound WT/L12-triple heterodimer kinesin (the L12-triple mutant (yellow spheres in **c**) cannot bind microtubules[24]). The 215 and 43 cysteine residues were introduced into wild-type and L12-triple heads, respectively (left) or into L12-triple and wild-type heads, respectively (right). Dotted lines are adopted from Fig. 1b. **b**, FRET histograms with 215/342 dyes on the wild-type chain (L12-triple chain is cysteine-light)[12] to probe neck-linker conformations in the bound head. The FRET efficiency peaks in the ADP/apyrase and AMP-PNP states are similar to those observed for the wild-type kinesin dimer with AMP-PNP (backward-extending and forward-extending (docked) neck linkers, respectively; Supplementary Fig. 8). **c**, Proposed model for the nucleotide-dependent configurations of the WT/L12-triple heterodimer, based on the FRET results.

heterodimer, the major FRET peak shifted in the opposite direction towards lower FRET efficiencies (Fig. 2a). These large nucleotide-dependent FRET changes suggest a movement of the L12-triple (unbound) head towards the plus-end-oriented tip (residue 215) of the wild-type (bound) head on binding of AMP-PNP (Fig. 2c). This translation of the unbound head from a rear position to a forward position is most probably driven by a nucleotide-dependent docking of the neck linker[8,9] in the bound head (Fig. 2b), the implications of which will be discussed later.

We next examined the smFRET signals for dimeric kinesin moving processively along a microtubule. At saturating ATP concentration (1 mM), we could measure only an average FRET efficiency of moving kinesin molecules, but could not accurately detect conformational transitions that might occur during kinesin stepping, because the stepping rate of kinesin (about $50\,s^{-1}$) is comparable to the camera acquisition rate (100 frames s^{-1}). The FRET efficiency for the 215–43 sensor showed a broad distribution centred at about 50% (Fig. 3a, b), a value consistent with an average of the bimodal 10%, 90% FRET distribution observed for static two-head-bound kinesin with AMP-PNP (and differing from the 30% value of one-head-bound kinesin, Fig. 1b). The 324–324 sensor yielded a unimodal FRET efficiency centred at about 30% with 1 mM ATP (Fig. 3a, b), which is also more similar to the distribution observed with the same FRET sensor with AMP-PNP than to that observed with ADP (Fig. 1b). Thus, the results from these two FRET sensors suggest that kinesin spends most of the time bound with two heads to the microtubule when moving at saturating ATP concentration (also see Supplementary Fig. 5), which is consistent with previously published fluorescence polarization measurements[22].

We next studied head–head smFRET at subsaturating ATP concentration (2 μM). When compared with the 1 mM ATP histograms, the main FRET efficiency peak for the 215–43 sensor shifted to about 30%, whereas the peak for the 324–324 sensor shifted to about 60% (Fig. 3a, b). These FRET distributions are more similar to those

observed with 200 nM ADP than to those observed with AMP-PNP (Fig. 1b). These results suggest that kinesin waits primarily as a one-head-bound intermediate when ATP binding becomes the rate-limiting step in the ATPase cycle.

With the longer dwell times at low ATP concentration, one might expect to observe FRET transitions that reveal how kinesin steps along the microtubule. At 2 μM ATP, moving 215–43 dye-labelled kinesin molecules ($n = 33$) spent most time in a roughly 30% FRET state (probably a one-head-bound state) with brief spikes (dwell time 34 ± 2 ms (mean ± s.e.m.)) towards higher (about 80%) FRET values (Fig. 3c, d, and Supplementary Figs 6 and 7). These higher FRET states could represent a transient two-head-bound intermediate state (similar to the 90% FRET state observed with AMP-PNP in which the 215-labelled head is in the trailing position; Fig. 1a, b). In this case, transitions from 30% to a lower FRET state (similar to the 10% FRET state with AMP-PNP) should also occur. Although such transitions were occasionally evident (Fig. 3c, arrowheads), the magnitude of such a FRET change is difficult to distinguish from the noise. However, the dwell times at the 30% FRET state (that is, the period between adjacent high-FRET spikes) provided additional support for the idea that transitions to both lower-FRET and higher-FRET states exist. This dwell-time histogram was best fitted by a convolution of two exponentials[7] (Fig. 3d, dotted line), suggesting that two rate-limiting ATP binding events occur between the two high-FRET spikes. Moreover, the mean dwell time derived from this double-exponential fit (140 ± 8 ms (mean ± s.e.m.)) is comparable to that predicted (160 ms) from the kinesin step size (8.3 nm)[4] and velocity at 2 μM ATP (51 ± 22 nm s^{-1}, $n = 33$). In addition, the total number of high FRET spikes from several single-molecule traces (272 spikes, $n = 33$) divided by the distance travelled by these molecules (4.57 μm) yielded an average travel distance of about 17 nm per high-FRET spike, which is close to double the kinesin step size (Fig. 3e). Collectively, these results suggest that a kinesin step at low ATP concentrations involves a short-lived, two-head-bound state (for
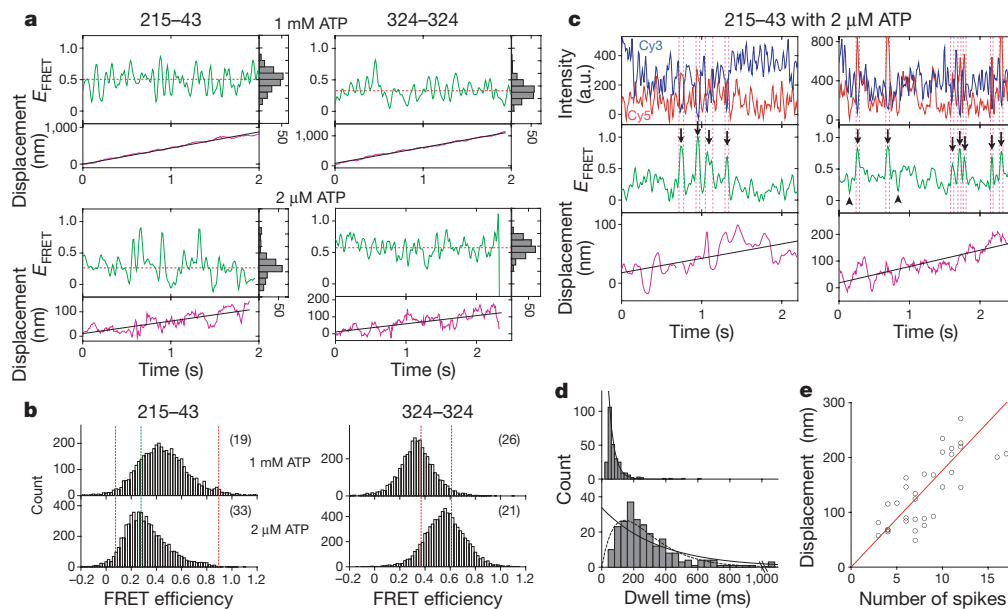
Figure 3 | Head–head configuration changes of kinesin while moving along microtubules. a, Examples of time traces of FRET efficiency, E_{FRET} (green; red dotted lines show the mean value; histogram at the right), and fluorophore centroid displacements (purple; black lines are a linear fit) of 215–43 or 324–324 dye-labelled kinesin moving along axonemes in the presence of 1 mM or 2 μM ATP. **b,** Histograms of FRET efficiencies (each frame) under the two different ATP conditions. Dotted lines are adopted from Fig. 1b. **c,** Typical traces of fluorescence intensities of donor (Cy3, blue) and acceptor (Cy5, red) fluorophores, FRET efficiency and axial displacement, for 215–43 heterodimer kinesin at 2 μM ATP, showing

transitions between one-head-bound and two-head-bound states. FRET changes greater than 0.3 are marked by vertical magenta dotted lines, with transitions towards high and low FRET states indicated by arrows and arrowheads, respectively. **d,** Distributions of dwell times in the high-FRET state (top) and between the high-FRET spikes (arrows in **c**) (bottom). Solid and dotted lines show single-exponential and double-exponential fits[7]. **e,** Relationship between number of transitions towards the high-FRET state and the displacement per observation time; each point represents a different single molecule. The solid red line shows a linear fit (17.6 nm per transition).

example, a high-FRET spike), which then undergoes a transition to a longer-lived, one-head-bound state (30% FRET state).

Whether kinesin waits as a one-head-bound or a two-head-bound intermediate between steps has been debated[13–16]. Our smFRET experiments suggest that both modes of movement are possible. At high ATP concentration (when the detachment of the trailing head— triggered by ATP hydrolysis/phosphate release—is likely to be rate-limiting[20]), kinesin moves hand-over-hand, making rapid transitions from one two-head-bound state to the next (Fig. 4a). However, when ATP binding to the lead, nucleotide-free, head becomes rate-limiting at low ATP concentrations (Fig. 4b), the trailing head releases its P_i and detaches from the microtubule, producing a long-lived one-head-bound configuration with the neck linkers in two different conformational states as described previously[12] (Supplementary Fig. 8). This latter pathway is a variation of the original model proposed by Rice et al.[8,9], with ATP binding to the leading head taking place after the transition to a one-head-bound state. Alonso et al.[21] recently proposed that kinesin waits between steps with the detached, ADP-bound head in front of the bound, nucleotide-free head. However, our FRET experiments with the WT/L12-triple heterodimer suggest that the detached head is located rearward on average, shifting to a forward position on binding of ATP to the bound head (Fig. 2). The rear positioning of the detached head also might explain an apparent inconsistency in the one-head waiting-state model with high spatial resolution tracking experiments[13–16], which showed an ATP-driven roughly 17-nm step of a kinesin head[7] (a distance

consistent with a detached head being positioned near the rear tubulin-binding site; Supplementary Fig. 9).

Our experiments also shed light on how the ATPase cycles in the two kinesin heads are coordinated during processive motion. The gating model of Alonso et al.[21] proposes that the detached head in the 'waiting state' is parked in front of the bound head but is in a conformation that prevents its binding to tubulin. However, transient interactions of the 'detached' head with the microtubule are seen in our low-ADP FRET data (Fig. 1c) and in ATPase kinetic measurements made by Hackney[23]. Thus, an additional mechanism must keep the detached head from progressing through its ATPase cycle until its partner head binds ATP. We suggest that the detached head, positioned behind the nucleotide-free, microtubule-bound head, will not release its bound ADP when it interacts with the rear tubulin-binding site. However, ADP release can occur after the detached head has been translated to a forward tubulin-binding site by ATP-triggered neck-linker docking in the bound partner head. This model is also supported by results from Guydosh & Block[26], who showed that nucleotide dissociation occurs only when a head is in the 'forward' position. We suggest that this position dependence in the ADP dissociation rate is controlled by the conformation of the neck linker, with a forward-pointing conformation of this mechanical element inhibiting ADP release in the trailing head (Fig. 4b). Further studies will be required for a better understanding of how structural states of the neck linker affect transitions in the ATPase cycle.

METHODS SUMMARY

DNA cloning and protein purification. Cysteine residues[12] and/or mutations[24] were introduced into a 'cysteine-light' human ubiquitous kinesin-1 dimer 490 amino-acid-residues long. Heterodimers were prepared by using a coexpression vector (one kinesin containing a carboxy-terminal streptavidin tag (Strep-tag) and the second with a His$_6$ tag) and purified by two-step affinity chromatography of nickel-nitrilotriacetic acid and Strep-Tactin[12]. Dialysed kinesin was reacted for 4 h at 4 °C with Cy3-maleimide and Cy5-maleimide at a motor head/Cy3 dye/Cy5 dye molar ratio of 1:10:10. Unreacted dyes were quenched with 1 mM dithiothreitol and then removed through microtubule affinity purification[12]. The 215–43 and 324–324 dual dye-labelled kinesins showed single-molecule processive movement with normal maximal velocity[27] (mean velocities at 1 mM ATP concentration were $410 \pm 60 \text{ nm s}^{-1}$ (mean ± s.d.; $n = 19$) for 215–43, and $430 \pm 80 \text{ nm s}^{-1}$ ($n = 26$) for 324–324), indicating that the substitutions, mutations and dye-labelling did not significantly alter motor activity.
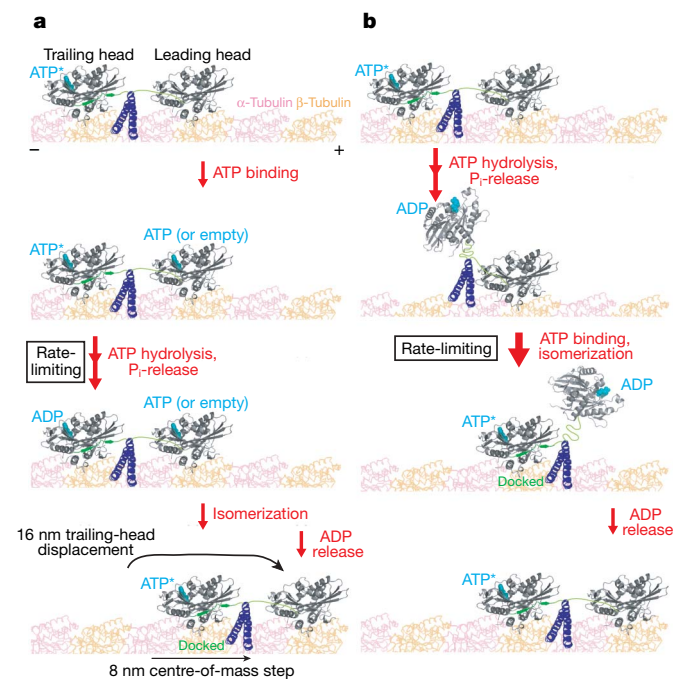
SmFRET. SmFRET measurements were performed with a custom-built prism-type laser-illuminated total-internal-reflection fluorescence microscope[12]. Dye-labelled kinesins were imaged either moving along sea-urchin axonemes in the presence of ATP and an ATP-regenerating system[12] or statically bound in the presence of AMP-PNP, ADP (5 U ml^{-1} hexokinase converted contaminating ATP (about 10 nM) to ADP), P_i (10 mM KH$_2$PO$_4$) or apyrase at about 22 °C. High concentrations (50 U ml^{-1}) of apyrase were required to deplete residual ATP and ADP (about 10 nM) completely; with a lower concentration (5 U ml^{-1}) of apyrase we observed a histogram distribution the peak value of which was intermediate between those with 50 U ml^{-1} apyrase and 200 nM ADP (that is, both one-head-bound and two-head-bound states).

Full Methods and any associated references are available in the online version of the paper at www.nature.com/nature.

Figure 4 | A model for kinesin motility. a, At high ATP concentrations, hydrolysis and phosphate release leading to trailing-head dissociation is rate-limiting (larger arrows represent slower steps). Once released, the trailing head is rapidly translated forwards by ATP isomerization-induced neck-linker docking in the partner head (indicated by ATP*), resulting in a rapid 8-nm step and a new two-head-bound intermediate. **b,** At low ATP concentrations, phosphate release occurs before the leading head binds an ATP molecule, producing a one-head-bound state in which the detached head is positioned behind the bound partner head. Although this head may interact transiently with the rear tubulin-binding site, we postulate that the conformation of the neck linker in this head is not compatible with ADP release and strong microtubule binding. Once ATP has bound to the forward head, the detached head translates forwards and, after a diffusional search, binds to a new tubulin subunit. ADP release from this head is now permitted by the backward-extending conformation of the neck linker in this two-head-bound state[12,22,23,28].

1. Vale, R. D. The molecular motor toolbox for intracellular transport. *Cell* **112**, 467–480 (2003).
2. Hirokawa, N. & Takemura, R. Molecular motors and mechanisms of directional transport in neurons. *Nature Rev. Neurosci.* **6**, 201–214 (2005).
3. Hackney, D. D. Evidence for alternating head catalysis by kinesin during microtubule-stimulated ATP hydrolysis. *Proc. Natl Acad. Sci. USA* **91**, 6865–6869 (1994).
4. Svoboda, K., Schmidt, C. F., Schnapp, B. J. & Block, S. M. Direct observation of kinesin stepping by optical trapping interferometry. *Nature* **365**, 721–727 (1993).
5. Asbury, C. L., Fehr, A. N. & Block, S. M. Kinesin moves by an asymmetric hand-over-hand mechanism. *Science* **302**, 2130–2134 (2003).
6. Kaseda, K., Higuchi, H. & Hirose, K. Alternate fast and slow stepping of a heterodimeric kinesin molecule. *Nature Cell Biol.* **5**, 1079–1082 (2003).
7. Yildiz, A., Tomishige, M., Vale, R. D. & Selvin, P. R. Kinesin walks hand-over-hand. *Science* **303**, 676–678 (2004).

8. Vale, R. D. & Milligan, R. A. The way things move: looking under the hood of molecular motor proteins. *Science* **288**, 88–95 (2000).
9. Rice, S. *et al.* A structural change in the kinesin motor protein that drives motility. *Nature* **402**, 778–784 (1999).
10. Skiniotis, G. *et al.* Nucleotide-induced conformations in the neck region of dimeric kinesin. *EMBO J.* **22**, 1518–1528 (2003).
11. Asenjo, A. B., Weinberg, Y. & Sosa, H. Nucleotide binding and hydrolysis induces a disorder–order transition in the kinesin neck-linker region. *Nature Struct. Mol. Biol.* **13**, 648–654 (2006).
12. Tomishige, M., Stuurman, N. & Vale, R. D. Single-molecule observations of neck linker conformational changes in the kinesin motor protein. *Nature Struct. Mol. Biol.* **13**, 887–894 (2006).
13. Carter, N. J. & Cross, R. A. Kinesin's moonwalk. *Curr. Opin. Cell Biol.* **18**, 61–67 (2006).
14. Valentine, M. T. & Gilbert, S. P. To step or not to step? How biochemistry and mechanics influence processivity in Kinesin and Eg5. *Curr. Opin. Cell Biol.* **19**, 75–81 (2007).
15. Hackney, D. D. Processive motor movement. *Science* **316**, 58–59 (2007).
16. Block, S. M. Kinesin motor mechanics: binding, stepping, tracking, gating, and limping. *Biophys. J.* **92**, 2986–2995 (2007).
17. Kawaguchi, K. & Ishiwata, S. Nucleotide-dependent single- to double-headed binding of kinesin. *Science* **291**, 667–669 (2001).
18. Uemura, S. *et al.* Kinesin-microtubule binding depends on both nucleotide state and loading direction. *Proc. Natl Acad. Sci. USA* **99**, 5977–5981 (2002).
19. Carter, N. J. & Cross, R. A. Mechanics of the kinesin step. *Nature* **435**, 307–312 (2005).
20. Auerbach, S. D. & Johnson, K. A. Alternating site ATPase pathway of rat conventional kinesin. *J. Biol. Chem.* **280**, 37048–37060 (2005).
21. Alonso, M. C. *et al.* An ATP gate controls tubulin binding by the tethered head of kinesin-1. *Science* **316**, 120–123 (2007).
22. Asenjo, A. B., Krohn, N. & Sosa, H. Configuration of the two kinesin motor domains during ATP hydrolysis. *Nature Struct. Biol.* **10**, 836–842 (2003).
23. Hackney, D. D. The tethered motor domain of a kinesin-microtubule complex catalyzes reversible synthesis of bound ATP. *Proc. Natl Acad. Sci. USA* **102**, 18338–18343 (2005).
24. Woehlke, G. *et al.* Microtubule interaction site of the kinesin motor. *Cell* **90**, 207–216 (1997).
25. Kaseda, K., Higuchi, H. & Hirose, K. Coordination of kinesin's two heads studied with mutant heterodimers. *Proc. Natl Acad. Sci. USA* **99**, 16058–16063 (2002).
26. Guydosh, N. R. & Block, S. M. Backsteps induced by nucleotide analogs suggest the front head of kinesin is gated by strain. *Proc. Natl Acad. Sci. USA* **103**, 8054–8059 (2006).
27. Tomishige, M., Klopfenstein, D. R. & Vale, R. D. Conversion of Unc104/KIF1A kinesin into a processive motor after dimerization. *Science* **297**, 2263–2267 (2002).
28. Sablin, E. P. & Fletterick, R. J. Coordination between motor domains in processive kinesins. *J. Biol. Chem.* **279**, 15707–15710 (2004).

METHODS

FRET imaging and data collection. Donor (Cy3) and acceptor (Cy5) dyes were excited with an argon laser (514 nm; 35LAP321; Melles Griot) and a diode laser (635 nm; Radius 635; Coherent Inc.), respectively. Fluorescence images from Cy3 and Cy5 (or FRET) were separated by using a Dual-View (Optical Insights) and then projected side-by-side on an electron-multiplying charge-coupled device camera (iXon DV860 DCS-BV; Andor). For the static FRET measurements, both Cy3 and Cy5 fluorophores were illuminated directly by sequential excitation with the argon laser (0.8 mW) and the laser diode (1.5 mW) at an acquisition rate of 50 frames s^{-1}. Both lasers were used to identify molecules that showed little or no FRET (to ensure that the acceptor dye was present but not being excited by the donor dye; an example is given in Supplementary Fig. 4)[12]. For the dynamic FRET measurements, images were taken by the excitation with the argon laser (3 mW) at an acquisition rate of 100 frames s^{-1}.

Data analysis. Images were analysed with Image J (http://rsb.info.nih.gov/ij/) with custom-designed plug-in software. For the static FRET measurements, we first identified Cy3–Cy5 dual-labelled motors on axonemes by using the time-averaged images (100 frames) for donor and acceptor excitations[12]. Axonemes that were sparsely coated with fluorescence spots (less than one spot per 2-μm microtubule) were used for data analysis to reduce the chance that two distinct Cy3 and Cy5 spots happened to localize together on the axonemes within one pixel (80 nm). Average FRET efficiencies were determined for each molecule as described previously[12]. FRET efficiencies were also determined for each frame (in both static and dynamic FRET measurements) as described previously[12], except that we first applied a three-frame gaussian filter to the intensity traces derived from raw images and further applied twice the three-frame gaussian filter to the calculated FRET efficiency traces. In the presence of AMP-PNP (under which conditions kinesin dimer stably takes a two-head-bound state), the FRET efficiency was fairly constant and we did not see transition during the observation time (about 5 s) (Fig. 1c and Supplementary Fig. 4). In this case, we used the averaged FRET efficiency of individual molecules to make histograms (only for those in Supplementary Fig. 2). In contrast, with other nucleotide conditions (ADP, ADP/P$_i$ and nucleotide-free) we often saw transitions (between one-headed and two-headed states). In these cases, FRET efficiency based on individual molecules does not properly represent individual states, so we used histograms based on individual frames to highlight each state that the kinesin dimer takes and its relative frequency (durations).

In the dynamic FRET measurements, the centroid positions of the fluorescence spots were tracked by using a gaussian fitting algorithm with images applied with ten-frame running averaging. Fluorescence spots that did not show clear unidirectional movement were not subjected to further data analysis. Transitions to a high-FRET-efficiency state ('spikes' for the 215–43 dye pair at 2 μM ATP) were identified manually as anticorrelated donor–acceptor intensity changes that accompanied FRET efficiency changes of more than 0.3. This cutoff amplitude of 0.3 was significantly greater than the noise level of FRET efficiency in our measurement with the acquisition rate of 100 frames s^{-1} (0.08 ± 0.02, $n = 20$), which was estimated as the s.d. of the FRET efficiency fluctuations in the traces for 43–215 dyes on one head[12] moving along axonemes in the presence of 2 μM ATP (Supplementary Fig. 6). The dwell time in the high-FRET state (Fig. 3d) was defined as the duration between the midpoints in the ascending and descending phases, and the dwell time in the median FRET state was defined as the duration between two adjacent transitions to the high-FRET state. The accuracy of determining the dwell time was about 10 ms (one frame).